RUVBL1 directly binds actin filaments and induces formation of cell protrusions to promote pancreatic cancer cell invasion

KEISUKE TANIUCHI[1], MUTSUO FURIHATA[2], SHINJI IWASAKI[3], KENJIRO TANAKA[1], TAKAHIRO SHIMIZU[1], MOTOAKI SAITO[1] and TOSHIJI SAIBARA[3]

Departments of [1]Pharmacology, [2]Pathology and [3]Gastroenterology and Hepatology, School of Medicine, Kochi University, Nankoku, Kochi 783-8505, Japan

Received February 24, 2014; Accepted March 28, 2014

DOI: 10.3892/ijo.2014.2380

Abstract. We report a novel function of RUVBL1 molecule in pancreatic cancer cells. Previous reports describe that RUVBL1 belongs to the family of AAA+ ATPases that associate with chromatin-remodelling complexes and have important roles in transcriptional regulation, the DNA damage response, telomerase activity and cellular transformation. We show that knockdown of RUVBL1 inhibited the motility and invasiveness of pancreatic cancer cells. RUVBL1 localized in the cytoplasm bound filamentous actin (F-actin) in cell protrusions, and increased concentration of monomeric globular-actin (G-actin) in cell protrusions of migrating pancreatic cancer cells. Cytoplasmic RUVBL1 functioned in additional formation of actin filaments in cell protrusions. Consequently, cytoplasmic RUVBL1 contributed to the formation of membrane protrusions by promoting peripheral actin polymerization. Our results imply that these RUVBL1-actin interactions could enhance the invasive properties of pancreatic cancer cells.

Introduction

RUVBL1 belongs to the family of AAA+ ATPases (ATPases associated with various cellular activities) associated with chromatin-remodelling complexes (1). RUVBL1 localized in the nucleus has intrinsic ATPase activity (2) and helicase activity with two ATP binding (Walker) sites (3). RUVBL1 is involved in many cellular processes that are highly relevant to cancer. RUVBL1 interacts with the oncogenes *c-Myc* (4) and *β-catenin* (5), and modulate their transcriptional activities. In cooperation with a member of the LEF/TCF family, β-catenin activates the transcription of a number of target genes relevant for cancer progression (6). Nuclear RUVBL1 participates in large molecular complexes such as the INO80 (7) or the TIP60 (8) complexes that are involved in chromatin remodeling or DNA damage repair. Nuclear RUVBL1 is also required for the biogenesis of telomerase (9). Findings from RNA interference (RNAi) or mutational analyses have indicated that RUVBL1 promotes cell growth and viability (10,11). Interestingly, an intact RUVBL1 ATPase domain is not essential for all RUVBL1 functions (12). Additionally, recent evidence indicates that RUVBL1 also has cytosolic functions such as regulation of nonsense-mediated decay of mRNAs (13). RUVBL1 is reportedly expressed on the extracellular surface of the plasma membrane of U937 monocytoid cells and peripheral blood monocytes, where it binds extracellular plasminogen and promotes activation of plasminogen into plasmin (14).

Cell motility is critical for a variety of biological processes in normal and pathological conditions; cell motility drives cellular development, tissue repair and cancer invasion and metastasis (15). The first step in cell motility is the generation of membrane protrusions in the direction of movement (16). Protrusion formation is driven by actin polymerization; specifically, monomeric globular-actin (G-actin) subunits form filamentous actin (F-actin) filaments (17). Protrusion formation probably also requires the addition of new membranes at the protrusion site. In motile processes, cells extend F-actin-rich protrusion; polarized, branched arrays of actin filaments within these protrusions are arranged with the fast-growing barbed ends near the plasma membrane and slow-growing pointed ends toward the rear (18). A highly polarized, dendritic network of F-actin polymerizes next to the plasma membrane of the leading edge; this network probably generates the forces that push the cell boundary forward (19,20).

Pancreatic ductal adenocarcinoma (PDAC) is among the deadliest cancers because PDAC cells are highly invasive, they easily invade surrounding tissues and they metastasize at an early stage (21). We previously reported that the formation of additional membrane protrusions increase the invasive and metastatic properties of the PDAC cells by regulating the activity of Rho GTPases [Rac1 (22) and RhoA (23)] and a protein kinase C [PKCα (24)]. The role of RUVBL1 in migration and invasion of cancer cells, including PDAC cells, has not been reported. Here, we sought to evaluate the role of RUVBL1 that

Correspondence to: Dr Keisuke Taniuchi, Department of Pharmacology, School of Medicine, Kochi University, Nankoku, Kochi 783-8505, Japan
E-mail: ktaniuchi@kochi-u.ac.jp

Key words: pancreatic ductal adenocarcinoma, AAA+ ATPase, invasiveness, cell protrusion, actin polymerization

localized in the cytoplasm in the control of PDAC cell motility and invasion. In the course of this investigation, we found that cytoplasmic RUVBL1 accumulated in membrane protrusions and in the leading edges of PDAC cells. Further investigation revealed that cytoplasmic RUVBL1 contributed to the formation of membrane protrusions; specifically, RUVBL1 promoted concentration of G-actin subunits and polymerization of actin filaments via its direct binding to F-actin in cell protrusions and results in increased invasive properties of PDAC cells.

Materials and methods

Antibodies. Anti-RUVBL1 antibody (H00008607-M01) was purchased from Abnova (Taipei, Taiwan, R.O.C.). JLA20 anti-actin antibody (MABT219) was purchased from Millipore (Temecula, CA). Anti-vitamin D-binding protein antibody (ab65636) was purchased from Abcam (Cambridge, MA).

Cell culture. The human PDAC cell line S2-013, a derivative of SUIT-2, was obtained from Dr T. Iwamura (Miyazaki Medical College, Miyazaki, Japan) (25). All cells were grown in Dulbecco's modified Eagle's medium (DMEM; Gibco-BRL, Carlsbad, CA) supplemented with 10% heat-inactivated fetal calf serum (FCS) at 37˚C in a humid atmosphere saturated with 5% CO_2.

siRNA treatments. A single mixture with four different short hairpin small interfering RNA (siRNA) oligonucleotides targeting *RUVBL1* was purchased from Qiagen (FlexiTube GeneSolution GS8607; Valencia, CA) and a single mixture with four different scrambled negative control siRNA oligonucleotides was obtained from Santa Cruz Biotechnology (37007; Santa Cruz, CA). To examine the effect of the siRNAs on *RUVBL1* expression, S2-013 and PANC-1 cells that expressed RUVBL1 were plated in 6-well plates. After 20 h, the cells were transfected with 80 pmols of each siRNA mixture in siRNA transfection reagent (Qiagen) following the manufacturer's instructions. After incubation for 48 h, cells were processed for western blot analysis, transwell motility or Matrigel invasion assays.

Immunoblot analysis of cell lysates. Each cell pellet was resuspended in 20 mM HEPES (pH 7.4), 100 mM KCl, 2 mM $MgCl_2$, 0.5% Triton X-100, protease inhibitor cocktail tablets (Roche, Penzberg, Germany) and phosphatase inhibitor cocktail (Nacalai, Kyoto, Japan). The bicinchoninic acid (BCA) assay was used to determine protein concentration in each lysate; an aliquot of each lysate was then diluted with sample buffer (50 mM Tris, 2% SDS, 0.1% bromophenol blue and 10% glycerol) to a final concentration of 1-2 μg/μl and analyzed by SDS-PAGE and western blot analysis.

Confocal immunofluorescence microscopy. Coverslips were treated with 10 μg/ml fibronectin (Sigma-Aldrich, St. Louis, MO) for 1 h at room temperature. Cells were seeded on fibronectin-coated glass coverslips and incubated for 5 h; cells were then fixed with 4% paraformaldehyde, permeabilized with 0.1% Triton X-100, covered with blocking solution (3% BSA/PBS), and then incubated with the primary antibody for 1 h. Alexa488- or Alexa594-conjugated secondary antibody (Molecular Probes, Carlsbad, CA) was used with or without rhodamine-conjugated phalloidin (Cytoskeleton, Denver, CO). Each specimen was visualized using a Zeiss LSM 510 META microscope (Carl Zeiss, Gottingen, Germany).

Immunostain wound-healing assay. A plastic pipette tip was used to cut cross-shaped wounds through a confluent cell monolayer; cells were then allowed to polarize and migrate into a wounded area. After 4 h, cells were immunostained with a primary antibody and then incubated with a fluorophore-conjugated secondary antibody as described above. Each specimen was examined using a Zeiss LSM 510 META microscope (Carl Zeiss).

Trans-well motility assay. Cells ($3.0x10^4$/chamber) were plated in the upper chamber of BD BioCoat Control Culture Inserts (24-well plates, 8-μm pore size; Becton-Dickinson, San Jose, CA). Serum-free culture medium was added to each upper chamber, and medium containing 5% FCS was added to each lower chamber. Cells were incubated on the membranes for 12 h. After this 12-h incubation, three independent visual fields in each lower chamber were examined via microscopic observation to count the number of cells that had moved from the top chamber to the lower chamber.

Matrigel invasion assay. A two-chamber invasion assay was used to assess PDAC cell invasiveness (24-well plates, 8-μm pore size membrane coated with a layer of Matrigel extracellular matrix proteins; Becton-Dickinson). Cells ($4.0x10^4$/chamber) suspended in serum-free medium were seeded into an upper chamber and allowed to invade towards a 5% FCS chemoattractant in a respective lower chamber. After 20-h incubation, three independent visual fields/lower chambers were examined via microscopic observation to count the number of cells that had moved to the bottom chamber.

Immunoprecipitation and mass spectrometric analysis of RUVBL1. S2-013 cells were seeded onto fibronectin and incubated for 5 h. Cells were lysed in lysis buffer [20 mM HEPES (pH 7.4), 100 mM KCl, 5 mM $MgCl_2$, 0.5% Triton X-100, protease inhibitor cocktail tablets (Roche), and phosphatase inhibitor cocktail (Nacalai)]. Lysates were immunoprecipitated with Dynabeads Protein G (Dynal, Oslo, Norway) and with anti-RUVBL1 antibody or normal mouse IgG (isotype control) for 2 h at 4˚C. Beads were pelleted on a magnetic rack (Dynal). Co-immunoprecipitated proteins were separated on a 4 to 20% gradient SDS-PAGE gel and then silver stained. Bands precipitated by the anti-RUVBL1 antibody were excised from the gel; a nano-LC MS/MS system, which consisted of an Ultimate HPLC system (Agilent 1100; Agilent Technologies, Santa Clara, CA) and a QSTAR XL mass spectrometer (Applied Biosystems/MDS SCIEX, Concord, ON, Canada) equipped with a nano-ESI source was used characterize the excised proteins (Genomine, Inc., Pohang, Korea). MASCOT v1.9.0 (Matrix Science, Boston, MA) was used to perform database searches with findings from the MS/MS spectra (Genomine, Inc.).

In vitro actin polymerization assay. Actin exists in equilibrium between monomeric subunits and polymeric filaments.

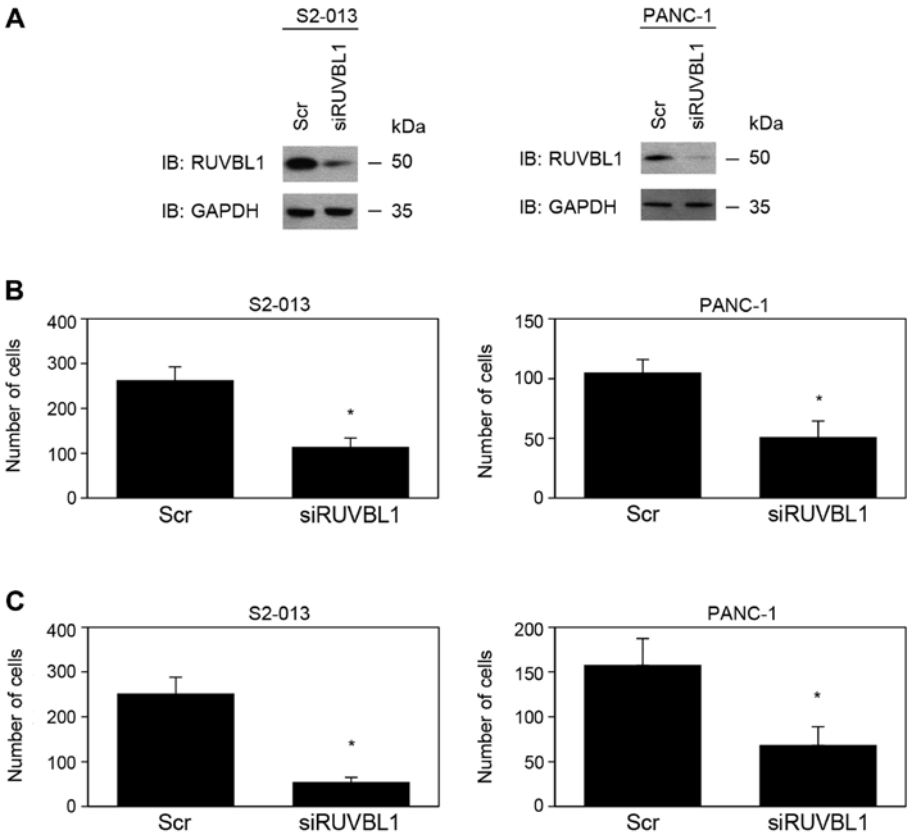

Figure 1. RUVBL1 promotes motility and invasion of PDAC cells. (A) A single mixture with four different siRNA oligonucleotides either targeting *RUVBL1* (siRUVBL1) or scrambled negative control (Scr) was transiently transfected into S2-013 and PANC-1 cells. Western blot analysis probed with anti-RUVBL1 antibody shows protein from the siRUVBL1 cells and the control Scr cells. (B) Transwell motility assay of control and RUVBL1 RNAi cells of S2-013 and PANC-1. For each treatment group, all migrating cells in four fields were scored. Data are derived from three independent experiments. Columns, mean; bars, SD. $^{*}p<0.02$ compared with scrambled control (Student's t-test). (C) Control and RUVBL1 RNAi cells of S2-013 and PANC-1 were seeded into Matrigel invasion chambers. For each treatment group, invading cells in four fields were counted. Data are derived from three independent experiments. Columns, mean; bars, SD. $^{*}p<0.005$ compared to scrambled control (Student's t-test).

To accurately quantify these actin forms, a commercially available actin polymerization assay (BK003; Cytoskeleton) was used to measure actin polymerization under defined conditions; specifically, polymerization-dependent increases in fluorescence of pyrene-conjugated actin were measured. Each of four concentrations (10, 30, 100 or 300 μg/ml) of recombinant human RUVBL1 protein (TP301170; Origene, Rockville, MD) were added to a separate actin polymerization assay. Briefly, the actin polymerization assays were based on the enhanced fluorescence of pyrene-conjugated actin that occurs during polymerization. The enhanced fluorescence was measured by pyrene monomer G-actin formed polymer pyrene F-actin in a fluorometer at excitation wavelength 365 nm and emission wavelength 407 nm. To quantify changes in polymerization rate, Boltzmann sigmoidal equations (GraphPad Prism version 6.0 software; GraphPad Software, Inc., La Jolla, CA) were used to fit curves to the fluorescence data. Half-maximal saturated polymerization values [$T^{1/2}$max (s)] were calculated from raw data.

Statistical analysis. GraphPad Prism version 6.0 software was used for all statistical analyses. Statistical significance was determined using a two-tailed Student's t-test and standard deviations. For all analyses, $p<0.05$ was considered significant.

Results

RUVBL1-knockdown reduces cell motility and invasion. To investigate whether RUVBL1 regulates cell growth, motility and invasion, RUVBL1 expression was suppressed by a single mixture with four different siRNA oligonucleotides against RUVBL1 in moderately differentiated PDAC cells (line S2-013) and the poorly differentiated PDAC cell line PANC-1 that endogenously expressed high levels of RUVBL1. Based on western blot data, RUVBL1 expression was markedly lower in *RUVBL1*-RNAi cells than in control cells 72 h after transfection of the respective siRNAs (Fig. 1A). RUVBL2 expression was not changed in *RUVBL1*-RNAi cells, compared to control cells (data not shown). These results indicated that *RUVBL1*-siRNAs specifically suppressed endogenous expression of RUVBL1 in S2-013 and PANC-1 cells. RNAi-mediated suppression of RUVBL1 did not affect cell growth in an *in vitro* MTT assay of S2-013 and PANC-1 (data not shown). Transwell motility and Matrigel invasion assays were used to examine the effect of RUVBL1 on cell motility and invasiveness. In Transwell motility assays, motility of S2-013 and PANC-1 cells was significantly lower in *RUVBL1*-RNAi cells than in control cells (Fig. 1B). In two-chamber invasion assays, invasiveness of *RUVBL1*-RNAi cells of S2-013 and PANC-1

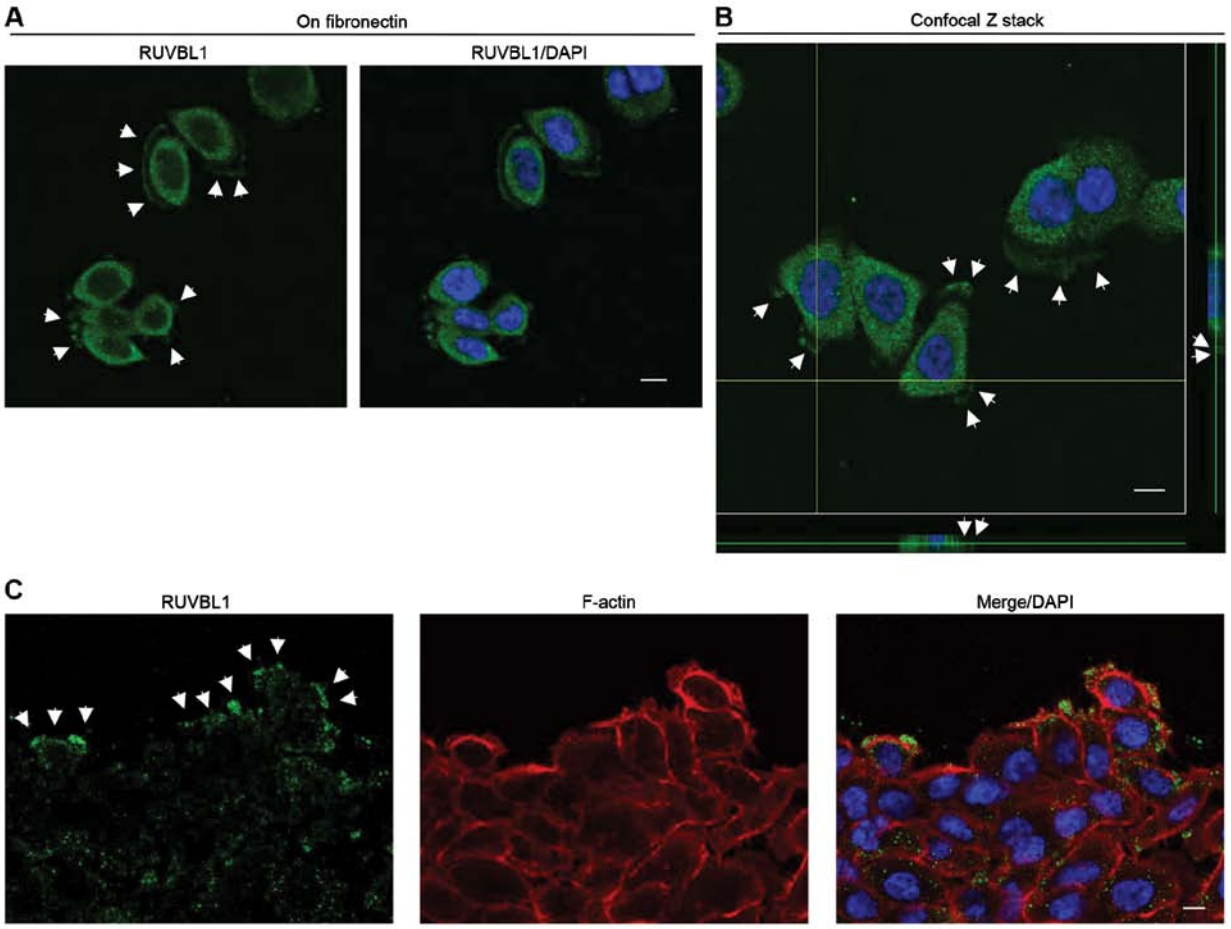

Figure 2. RUVBL1 localizes in plasma membrane protrusions of spreading PDAC cells. (A) S2-013 cells were cultured on fibronectin and then labeled with anti-RUVBL1 antibody (green). Arrows, RUVBL1 localized in cell protrusions. Blue, DAPI staining. Bar, 10 μm. (B) Confocal Z stack shows nuclear DAPI staining (blue) and the accumulation of RUVBL1 (green) in membrane protrusions of S2-013 cells. Arrowheads, RUVBL1 localized in cell protrusions. The lower and right panels in the confocal Z stack show a vertical cross-section (yellow lines) through the cells. Bar, 10 μm. (C) A confluent S2-013 cell monolayer was wounded. After 4 h, anti-RUVBL1 antibody (green) and phalloidin (red) were used to label the cells. Arrowheads, RUVBL1 at the leading edges of migrating cells. Blue, DAPI staining. Bar, 10 μm.

was significantly lower than that of control cells (Fig. 1C). These results indicated that RUVBL1 promoted the motility and invasiveness of PDAC cells.

RUVBL1 localizes in cell protrusion of migrating PDAC cells. Endogenous RUVBL1 localizes with transcription factors mainly to the nucleus, and regulates its target genes including *p53* in colon cancer cells (26). We used immunocytochemistry to determine the subcellular localization of RUVBL1 in S2-013 cells. Notably, when S2-013 cells that were initially in suspension attach to an immobilized fibronectin substrate, nascent membrane protrusions (*de novo* formation of actin patches at the cell periphery) form, and as these protrusions mature, they promote cell motility and invasion (22). Therefore, we analyzed the subcellular distribution of RUVBL1 in PDAC cells cultured on fibronectin. Spreading of S2-013 cells on fibronectin promoted accumulation of cytoplasmic RUVBL1 in membrane protrusions (Fig. 2A). These results indicated that the function of cytoplasmic RUVBL1 may be different from that of nuclear RUVBL1 in PDAC cells. Z stack panels substantiated this result in S2-013 cells cultured on fibronectin (Fig. 2B). Additionally, an immunostaining wound-healing assay was used to analyze localization of RUVBL1 in polarized migrating S2-013 cells; results from this assay showed that RUVBL1 was recruited to the leading edges, in which peripheral actin structures were abundant, during wound healing (Fig. 1C). Additionally, an immunostaining wound-healing assay was used to analyze localization of RUVBL1 in polarized migrating S2-013 cells (Fig. 2C); results from this assay showed that cytoplasmic RUVBL1 was recruited to the leading edges of S2-013 cells during wound healing. Based on these results, we reasoned that localization of RUVBL1 in membrane protrusions may be important to cell motility and invasiveness.

RUVBL1 associates with actin filaments. To investigate the mechanism by which RUVBL1 promoted cell motility and invasiveness, immunoprecipitation (IP) experiments were performed with lysates from fibronectin-stimulated S2-013 cells; a specific anti-RUVBL1 antibody was used to detect multiprotein complexes that contained RUVBL1. Control and anti-RUVBL1 immunoprecipitates were subject to SDS-PAGE; the separated proteins were silver stained. A 40-kDa band was evident in the anti-RUVBL1 sample that was very weak in

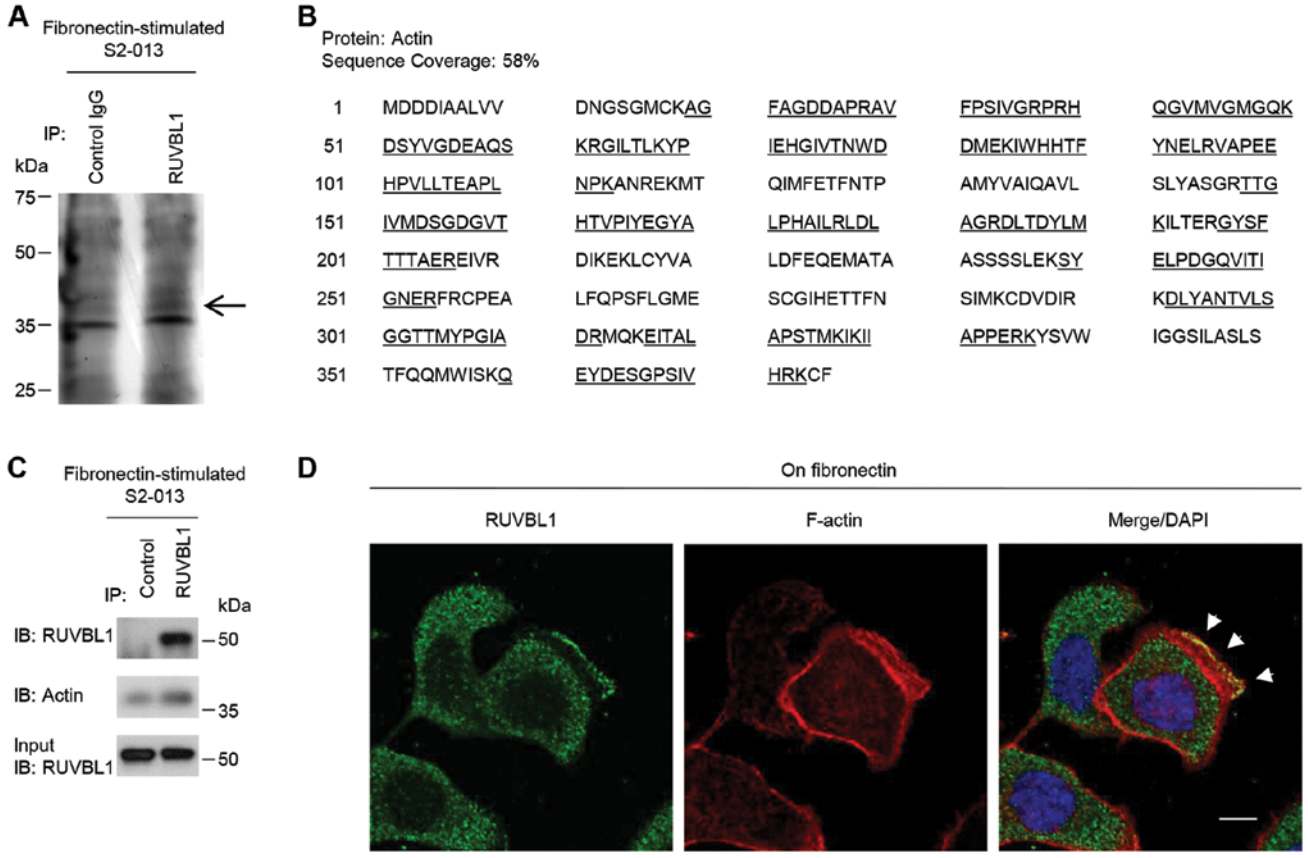

Figure 3. RUVBL1 associates with F-actin in cell protrusions. (A) Immunoprecipitates from fibronectin-stimulated S2-013 cells using control mouse IgG monoclonal antibody and anti-RUVBL1 monoclonal antibody were examined by silver stain analysis. A 40-kDa band is indicated by an arrow. (B) Percent coverage for actin is represented by the identified peptides in the total protein sequence (accession no. NP_001092). (C) IP of RUVBL1 from S2-013 cells cultured on fibronectin. Proteins within immunoprecipitates were examined on western blots probed with antibodies against RUVBL1 and actin. Control mouse IgG monoclonal antibody was used as an isotype control. (D) Immunocytochemical staining of S2-013 cells cultured on fibronectin; anti-RUVBL1 (green) antibody and phalloidin (red) were used to label endogenous proteins. Arrowheads, RUVBL1 colocalized with F-actin in cell protrusions. Blue, DAPI staining. Bar, 10 μm.

the isotype control sample (Fig. 3A). The band was excised, and LC-MS/MS was used to identify the constituent protein after in-gel trypsin digestion; the protein was actin. The peptide sequence coverage was 58% (Fig. 3B). Immunoblot analysis showed that a faint band of actin was detected in control-immunoprecipitates from fibronectin-stimulated S2-013 cells (Fig. 3C), suggesting the presence of low levels of non-specific actin in all IP samples. Strong actin band was detected in the anti-RUVBL1-immunoprecipitates (Fig. 3C), indicating that actin was enriched in RUVBL1-IP materials compared to control IgG-IPs.

Immunocytochemical signal from RUVBL1 and fluorescent signal from peripheral F-actin structures (labeled by phalloidin) were colocalized in cell protrusions of fibronectin-stimulated S2-013 cells (arrowheads in Fig. 3D). Thus, we hypothesized that the RUVBL1-actin complexes localized in cell protrusions could function in promotion of the motility and invasiveness.

Effects of RUVBL1 on in vitro actin polymerization. To investigate whether RUVBL1 influenced the structural organization of F-actin, we assessed whether RUVBL1 had an effect on the apparent rate of actin polymerization. Actin polymerization was monitored using an *in vitro* pyrene-labeled G-actin polymerization assay. The kinetics of actin polymerization in the presence of 30, 100 or 300 μg/ml RUVBL1 was measured by increase in pyrene fluorescence (Fig. 4A). Half-maximal saturated polymerization values [$T^{1/2}$max (s)] calculated from Boltzmann sigmoidal curve fits are summarized in Fig. 4B. It is likely that $T^{1/2}$max values for actin reactions in the presence of 30, 100 or 300 μg/ml RUVBL1 were faster than that in vehicle control. A significant difference in synergistic polymerization rates between vehicle control and added RUVBL1 became evident at a time point of 60 min (Fig. 4C). In contrast, RUVBL1 had no discernible effect on the kinetics of *in vitro* pyrene-labeled F-actin depolymerisation assays that involved measurement of F-actin fluorescence (Fig. 4D). These results indicated that binding of RUVBL1 to F-actin enhanced elongation of existing actin filaments.

Effects of RUVBL1 on G-actin concentration in cell protrusions. Immunocytochemistry and an antibody against vitamin D-binding protein [DBP (27)], a protein that specifically binds G-actin, was used to indirectly assess the presence and localization of G-actin in fibronectin-stimulated S2-013 cells; the cells had transfected with either scrambled control-siRNA or RUVBL1-siRNA. In control cells, G-actin accumulated in cell protrusions of motile cells (arrows in Fig. 5A); notably,

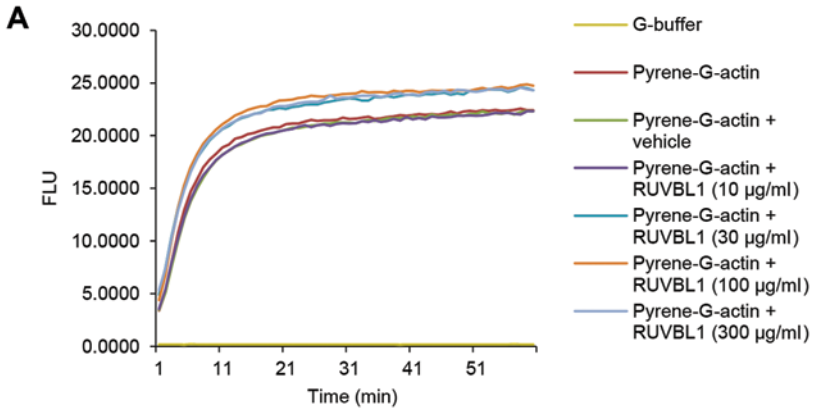

B

Condition	$T^{1/2}$max (s)
G-buffer	No fit
Pyrene-G-actin	245.94 ± 12.54
Pyrene-G-actin + vehicle	273.42 ± 11.97
Pyrene-G-actin + RUVBL1 (10 µg/mL)	259.50 ± 11.20
Pyrene-G-actin + RUVBL1 (30 µg/mL)	209.22 ± 7.230
Pyrene-G-actin + RUVBL1 (100 µg/mL)	211.86 ± 9.91
Pyrene-G-actin + RUVBL1 (300 µg/mL)	212.94 ± 7.60

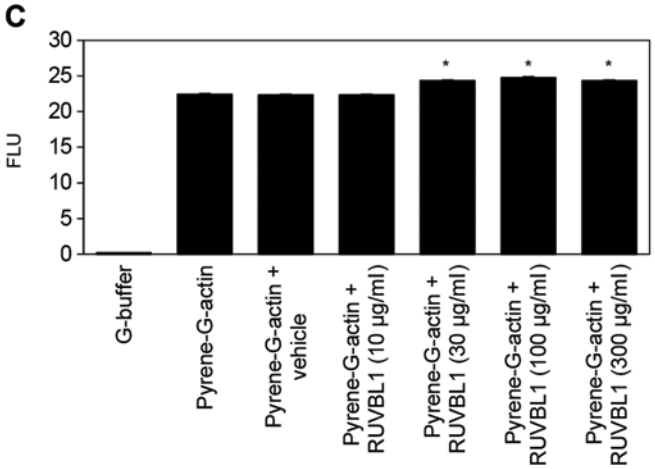

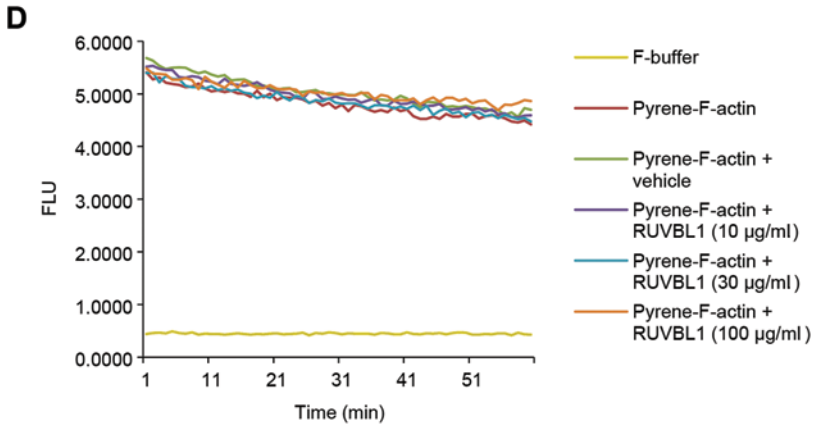

Figure 4. RUVBL1 induces actin polymerization *in vitro*. (A) The effect of RUVBL1 on actin polymerization kinetics was measured by observing the change in pyrene-labeled actin fluorescence during polymerization of G-actin in the presence or absence of recombinant RUVBL1 (10-300 μg/ml). (B) To quantify changes in polymerization in (A), curves were fitted with Boltzmann sigmoidal equations (GraphPad Prism). Half-maximal saturated polymerization times [$T^{1/2}$max (s)] are plotted. (C) Quantification of actin polymerization in (A). ABS on y-axis means absorbance at 60 min-time point. Data are derived from three independent experiments. Columns, mean; bars, SD. *p<0.001 indicate statistical significance calculated by Student's t-test. (D) Effect of increasing amounts of added recombinant RUVBL1 (10-100 μg/ml) on depolymerization of pyrene-actin as compared with buffer alone and with PBS-vehicle control. Depolymerization was determined according to increasing pyrene fluorescence during depolymerization of F-actin.

RUVBL1 and peripheral F-actin filaments were colocalized in these cell protrusions (Fig. 3D), but RUVBL1 did not bind to G-actin in these control protrusions (Fig. 5A). In contrast, siRNA-mediated suppression of RUVBL1 inhibited the accumulation of G-actin near the cell membranes (Fig. 5B). A significant difference in rates of G-actin concentration in cell protrusion between scrambled control and knockdown of RUVBL is shown in Fig. 5C. Suppression of RUVBL1 decreased G-actin concentration in the protrusion of S2-013. These results indicated that RUVBL1 played a role in induction of G-actin concentration in cell protrusions.

RUVBL1 induces the formation of membrane protrusions. We analyzed peripheral F-actin structures in membrane ruffles of S2-013 cells transfected with scrambled control or RUVBL1 siRNA; all cells were cultured on fibronectin. Knockdown of RUVBL1 inhibited the increase in peripheral F-actin structures compared to control cells (Fig. 6A). To determine whether

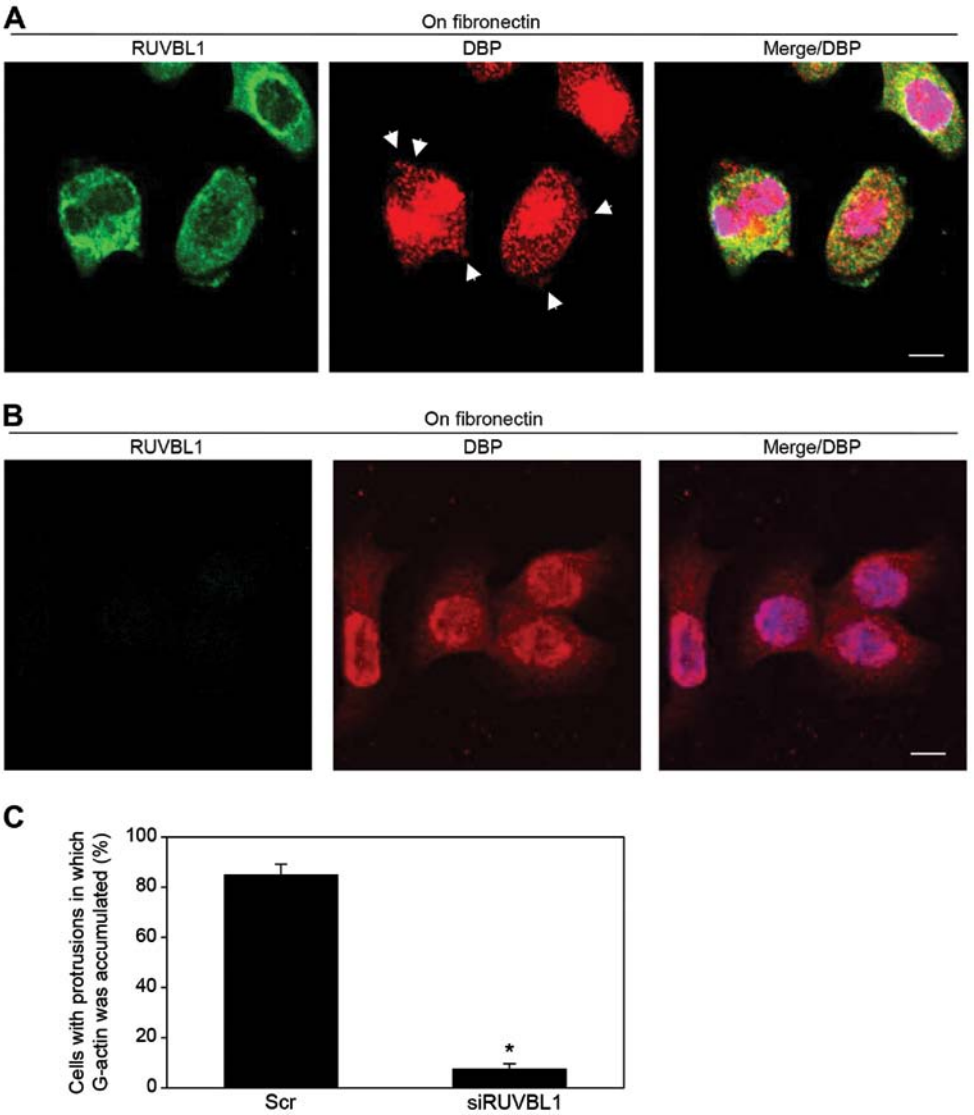

Figure 5. RUVBL1 associates with G-actin concentration in cell protrusions. (A) S2-013 cells treated with scrambled control siRNA were incubated on fibronectin and immunocytochemically labeled with anti-RUVBL1 (green) and anti-DBP (red) antibodies. Arrowheads, G-actin concentrated in cell protrusions. Blue, DAPI staining. Bar, 10 μm. (B) *RUVBL1*-knockdown S2-013 cells were incubated on fibronectin and immunocytochemically labeled with anti-RUVBL1 (green) and anti-DBP (red) antibodies. Blue, DAPI staining. Bar, 10 μm. (C) Quantification of data shown in (A) and (B); the values represent the number of scrambled control S2-013 cells or *RUVBL1*-knockdown S2-013 cells with cell protrusions in which G-actin was concentrated. For each treatment group, all cells in four fields were scored. Data derived from three independent experiments. Columns, mean; bars, SD. $^{*}p<0.001$ compared with control cells (Student's t-test).

RUVBL1 that increased F-actin structures in cell protrusions has a role in inducing membrane protrusions, immunofluorescence was carried out; all cells were treated with either scrambled control or RUVBL1 RNAi and cultured on fibronectin. siRNA-mediated suppression of RUVBL1 significantly inhibited the formation of fibronectin-mediated membrane protrusions in which peripheral actin structures were abundant, compared to scrambled control (Fig. 6B). These results indicated that RUVBL1 induced peripheral F-actin polymerization in cell protrusions that promoted formation of cell protrusions, and that these RUVBL1-mediated actin rearrangements promote the motility and invasiveness of PDAC cells.

Discussion

RUVBL1 is overexpressed in a variety of human solid tumors including, colorectal (28), gastric (29), bladder (30) and non-small cell lung (31) cancers. As noted in the Introduction, RUVBL1 is an ATPase protein that is associated with several chromatin-remodelling complexes in the nucleus. RUVBL1 localized in the nucleus promotes histone H3K9 trimethylation and negatively regulates p53 expression in colon cancer cells (26). Substantial evidence clearly demonstrates that RUVBL1 localized in the nucleus is required for cell growth and viability (32,33); however, the role of RUVBL1 in motility and invasion of cancer cells has not been fully examined. Here, we found that RUVBL1 localized mainly to the cytoplasm and some population of cytoplasmic RUVBL1 accumulated in cell protrusions of PDAC cells. We describe a newly discovered function for RUVBL1 localized at cell protrusions in cell motility and invasion in PDAC. RUVBL1 played a role as an F-actin-binding protein in mediating actin polymerization, but it did not interact with G-actin. Notably, RUVBL1 enhanced elongation of existing actin filaments via the direct binding

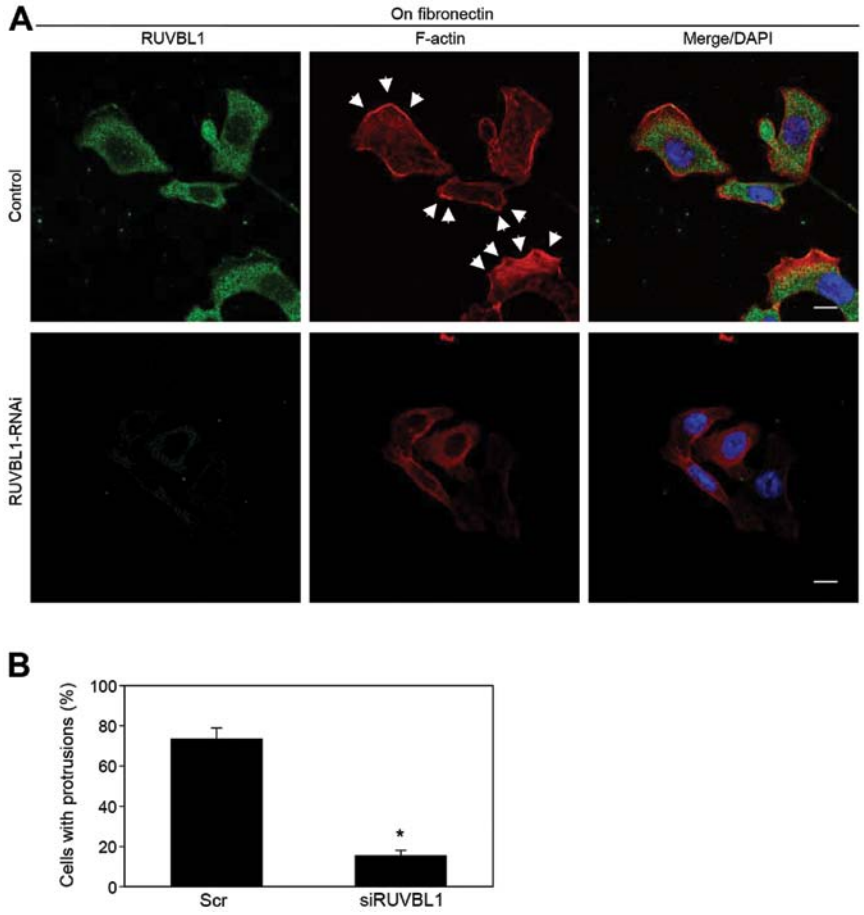

Figure 6. RUVBL1 accumulated in cell protrusions induces the formation of additional membrane protrusions. (A) S2-013 cells treated with scrambled control or *RUVBL1* siRNA were incubated on fibronectin and immunocytochemically stained with anti-RUVBL1 antibody (green) and phalloidin (red). Arrows, F-actin localized in cell protrusions of control cells. Blue, DAPI staining. Bars, 10 μm. (B) Quantification of data shown in (A); the values represent the number of scrambled control S2-013 cells or RUVBL1-knockdown S2-013 cells with cell protrusions in which peripheral actin structures were increased. For each treatment group, all cells in four fields were scored. Data are derived from three independent experiments. Columns, mean; bars, SD. *p<0.001 compared with control cells (Student's t-test).

to F-actin in cell protrusions of spreading PDAC cells. PDAC cells depend on actin-based motility to invade nearby organs such as the duodenum, stomach or liver (34). Knockdown of RUVBL1 inhibited the formation of cell protrusions via decrease in peripheral actin rearrangements. Suppression of RUVBL1 did not affect cell growth in an *in vitro* MTT assay using S2-013 and PANC-1 (data not shown); therefore, it is likely that cytoplasmic RUVBL1 was associated with actin-based motility and invasiveness of PDAC cells.

G-actin is the building block for F-actin, and local concentrations of G-actin directly affect the rate of filament assembly (35). Cell protrusions produced in motile cells contain G-actin (36), but whether spatio-temporal regulation of G-actin is important to cancer cell motility and invasion is unknown. We examined the intracellular distribution of G-actin and of F-actin in RNAi-treated S2-013 cells; all cells were treated with either scrambled control or RUVBL1 RNAi and cultured on fibronectin. G-actin was abundantly localized to membrane protrusions in scrambled control cells, whereas the peripheral concentration of G-actin was inhibited by suppression of RUVBL1 (Fig. 5A-C). RUVBL1 was associated with polymerization of G-actin, but it failed to depolymerize F-actin in *in vitro* assays (Fig. 4A-D); therefore, RUVBL1 was probably involved in the spatial arrangement of G-actin and its localization to membrane protrusions, resulted in increased F-actin structures in the protrusions. These results indicate that reductions in G-actin concentration were tightly associated with cessation and retraction of actin polymerization (Fig. 6A) and membrane protrusions (Fig. 6B) in RUVBL1 RNAi cells. Consistent with our findings, the concentration of G-actin in cell protrusions is sufficiently high to support actin polymerization at the tip of the cell protrusions in breast cancer cells (37).

Crawling cells typically move over substrates by the combined effects of i) actin-based protrusions at leading cell edges; ii) adhesion to the substrate; and iii) myosin-based contraction at the cell rear (38). Dynamic, actin-based plasma membrane protrusions that control growth cone path-finding include i) lamellipodia in which the actin cytoskeleton assumes a crosslinked and branched meshwork; and ii) filopodia, which consist of parallel bundles of actin filaments protruding from the growth cone or lamellipodial margin (39). Migratory competence of tumor cells requires activation of the motile cycle, the first step of which is actin remodeling;

this remodeling drives the formation of cell protrusions, defines the direction of migration, and initiates the growth of the lamellipodium (40). In this study, fibronectin-stimulated peripheral actin rearrangements and subsequent formation of membrane protrusions were inhibited when RUVBL1 RNAi S2-013 cells were plated on fibronectin. Thus, RUVBL1, which associates with F-actin filaments, is probably a physiological activator that induces peripheral actin rearrangements, which themselves promote formation of membrane protrusions.

The findings presented in this report are consistent with the hypothesis that RUVBL1 that localized in cell protrusions has pivotal roles in the coordinated regulation of cortical actin changes via the direct binding to F-actin. We have established the functional significance of RUVBL1 and that RUVBL1-mediated actin polymerization promoted i) the spatio-temporal localization of G-actin to protrusions, and ii) the formation of additional membrane protrusions in motile PDAC cells; the RUVBL1-mediated actin polymerization may play an important role in PDAC motility and invasiveness. Inhibition of binding between RUVBL1 and actin filaments may be a rational approach to a targeted molecular therapy for PDAC because such a therapy would inhibit the formation of cell protrusions and consequently limit the motility and invasiveness of PDAC cells.

Acknowledgements

We thank Aki Tanouchi and Chiaki Okura for their excellent technical assistance. This study was supported by the Grants-in-Aid for Scientific Research (KAKENHI) (to K.T. and S.I.), by the Pancreas Research Foundation of Japan (to K.T.), and by the Japanese Foundation for Multidisciplinary Treatment of Cancer (to K.T.).

References

1. Ammelburg M, Frickey T and Lupas AN: Classification of AAA+ proteins. J Struct 156: 2-11, 2006.
2. Kanemaki M, Kurokawa Y, Matsuura T, Makino Y, Masani A, Okazaki K, Morishita T and Tamura TA: TIP49b, a new RuvB-like DNA helicase, is included in a complex together with another RuvB-like DNA helicase, TIP49a. J Biol Chem 274: 22437-22444, 1999.
3. Qiu XB, Lin YL, Thome KC, Pian P, Schlegel BP, Weremowicz S, Parvin JD and Dutta A: An eukaryotic RuvB-like protein (RUVBL1) essential for growth. J Biol Chem 273: 27786-27793, 1998.
4. Wood MA, McMahon SB and Cole MD: An ATPase/helicase complex is an essential cofactor for oncogenic transformation by c-Myc. Mol Cell 5: 321-330, 2000.
5. Bauer A, Chauvet S, Huber O, Usseglio F, Rothbacher U, Aragnol D, Kemler R and Pradel J: Pontin52 and reptin52 function as antagonistic regulators of beta-catenin signalling activity. EMBO J 19: 6121-6130, 2000.
6. Hoverter NP and Waterman ML: A Wnt-fall for gene regulation: repression. Sci Signal 1: e43, 2008.
7. Ni L, Saeki M, Xu L, Nakahara H, Saijo M, Tanaka K and Kamisaki Y: RPAP3 interacts with Reptin to regulate UV-induced phosphorylation of H2AX and DNA damage. J Cell Biochem 106: 920-928, 2009.
8. Ikura T, Ogryzko VV, Grigoriev M, Groisman R, Wang J, Horikoshi M, Scully R, Qin J and Nakatani Y: Involvement of the TIP60 histone acetylase complex in DNA repair and apoptosis. Cell 102: 463-473, 2000.
9. Venteicher AS, Meng Z, Mason PJ, Veenstra TD and Artandi SE: Identification of ATPases pontin and reptin as telomerase components essential for holoenzyme assembly. Cell 132: 945-957, 2008.
10. Rousseau B, Ménard L, Haurie V, Taras D, Blanc JF, Moreau-Gaudry F, Metzler P, Hugues M, Boyault S, Lemière S, Canron X, Costet P, Cole M, Balabaud C, Bioulac-Sage P, Zucman-Rossi J and Rosenbaum J: Overexpression and role of the ATPase and putative DNA helicase RuvB-like 2 in human hepatocellular carcinoma. Hepatology 46: 1108-1118, 2007.
11. Ménard L, Taras D, Grigoletto A, Haurie V, Nicou A, Dugot-Senant N, Costet P, Rousseau B and Rosenbaum J: In vivo silencing of Reptin blocks the progression of human hepatocellular carcinoma in xenografts and is associated with replicative senescence. J Hepatol 52: 681-689, 2010.
12. Grigoletto A, Lestienne P and Rosenbaum J: The multifaceted proteins reptin and pontin as major players in cancer. Biochim Biophys Acta 1815: 147-157, 2011.
13. Izumi N, Yamashita A, Iwamatsu A, Kurata R, Nakamura H, Saari B, Hirano H, Anderson P and Ohno S: AAA+ proteins RUVBL1 and RUVBL2 coordinate PIKK activity and function in nonsense-mediated mRNA decay. Sci Signal 23: ra27, 2010.
14. Hawley SB, Tamura T and Miles LA: Purification, cloning, and characterization of a profibrinolytic plasminogen-binding protein, TIP49a. J Biol Chem 276: 179-186, 2001.
15. Ridley AJ: Rho GTPases and cell migration. J Cell Sci 114: 2713-2722, 2001.
16. Totsukawa G, Wu Y, Sasaki Y, Hartshorne DJ, Yamakita Y, Yamashiro S and Matsumura F: Distinct roles of MLCK and ROCK in the regulation of membrane protrusions and focal adhesion dynamics during cell migration of fibroblasts. J Cell Biol 164: 427-439, 2004.
17. Pollard TD, Blanchoin L and Mullins RD: Molecular mechanisms controlling actin filament dynamics in nonmuscle cells. Annu Rev Biophys Biomol Struct 29: 545-576, 2000.
18. Wang W, Goswami S, Sahai E, Wyckoff JB, Segall JE and Condeelis JS: Tumor cells caught in the act of invading: their strategy for enhanced cell motility. Trends Cell Biol 15: 138-145, 2005.
19. Pollard TD and Borisy GB: Cellular motility driven by assembly and disassembly of actin filaments. Cell 112: 453-465, 2003.
20. Ponti A, Matov A, Adams M, Gupton S, Waterman-Storer CM and Danuser G: Periodic patterns of actin turnover in lamellipodia and lamellae of migrating epithelial cells analyzed by quantitative Fluorescent Speckle Microscopy. Biophys J 89: 3456-3469, 2005.
21. Baumgart M, Heinmöller E, Horstmann O, Becker H and Ghadimi BM: The genetic basis of sporadic pancreatic cancer. Cell Oncol 27: 3-13, 2005.
22. Taniuchi K, Yokotani K and Saibara T: BART inhibits pancreatic cancer cell invasion by Rac1 inactivation through direct binding to active Rac1. Neoplasia 14: 440-450, 2012.
23. Taniuchi K, Iwasaki S and Saibara T: BART inhibits pancreatic cancer cell invasion by inhibiting ARL2-mediated RhoA inactivation. Int J Oncol 39: 1243-1252, 2011.
24. Taniuchi K, Yokotani K and Saibara T: BART inhibits pancreatic cancer cell invasion by PKCα inactivation through binding to ANX7. PLoS One 7: e35674, 2012.
25. Iwamura T, Katsuki T and Ide K: Establishment and characterization of a human pancreatic cancer cell line (SUIT-2) producing carcinoembryonic antigen and carbohydrate antigen 19-9. Jpn J Cancer Res 78: 54-62, 1987.
26. Taniue K, Oda T, Hayashi T, Okuno M and Akiyama T: A member of the ETS family, EHF, and the ATPase RUVBL1 inhibit p53-mediated apoptosis. EMBO Rep 12: 682-689, 2011.
27. Meijerman I, Blom WM, de Bont HJ, Mulder GJ and Nagelkerke JF: Changes of G-actin localisation in the mitotic spindle region or nucleus during mitosis and after heat shock: a histochemical study of G-actin in various cell lines with fluorescent labelled vitamin D-binding protein. Biochim Biophys Acta 1452: 12-24, 1999.
28. Ki DH, Jeung HC, Park CH, Kang SH, Lee GY, Lee WS, Kim NK, Chung HC and Rha SY: Whole genome analysis for liver metastasis gene signatures in colorectal cancer. Int J Cancer 121: 2005-2012, 2007.
29. Li W, Zeng J, Li Q, Zhao L, Liu T, Björkholm M, Jia J and Xu D: Reptin is required for the transcription of telomerase reverse transcriptase and over-expressed in gastric cancer. Mol Cancer 9: 132, 2010.
30. Dyrskjøt L, Kruhøffer M, Thykjaer T, Marcussen N, Jensen JL, Møller K and Ørntoft TF: Gene expression in the urinary bladder: a common carcinoma in situ gene expression signature exists disregarding histopathological classification. Cancer Res 64: 4040-4048, 2004.

31. Dehan E, Ben-Dor A, Liao W, Lipson D, Frimer H, Rienstein S, Simansky D, Krupsky M, Yaron P, Friedman E, Rechavi G, Perlman M, Aviram-Goldring A, Izraeli S, Bittner M, Yakhini Z and Kaminski N: Chromosomal aberrations and gene expression profiles in non-small cell lung cancer. Lung Cancer 56: 175-184, 2007.
32. Ducat D, Kawaguchi S, Liu H, Yates JR III and Zheng Y: Regulation of microtubule assembly and organization in mitosis by the AAA+ ATPase pontin. Mol Biol Cell 19: 3097-3110, 2008.
33. Schlabach MR, Luo J, Solimini NL, Hu G, Xu Q, Li MZ, Zhao Z, Smogorzewska A, Sowa ME, Ang XL, Westbrook TF, Liang AC, Chang K, Hackett JA, Harper JW, Hannon GJ and Elledge SJ: Cancer proliferation gene discovery through functional genomics. Science 319: 620-624, 2008.
34. Kedrin D, van Rheenen J and Segall JE: Cell motility and cytoskeletal regulation in invasion and metastasis. J Mammary Gland Biol 12: 143-152, 2007.
35. Lee CW, Vitriol EA, Shim S, Wise AL, Velayutham RP and Zheng JQ: Dynamic localization of G-actin during membrane protrusion in neuronal motility. Current Biology 23: 1046-1056, 2013.
36. Van Goor D, Hyland C, Schaefer AW and Forscher P: The role of actin turnover in retrograde actin network flow in neuronal growth cones. PLoS One 7: e30959, 2012.
37. Kiuchi T, Nagai T, Ohashi K and Mizuno K: Measurements of spatiotemporal changes in G-actin concentration reveal its effect on stimulus-induced actin assembly and lamellipodium extension. J Cell Biol 193: 365-380, 2011.
38. Mogilner A and Keren K: The shape of motile cells. Curr Biol 19: R762-R771, 2009.
39. Gallo G and Letourneau PC: Regulation of growth cone actin filaments by guidance cues. J Neurobiol 58: 92-102, 2004.
40. Eiseler T, Döppler H, Yan IK, Kitatani K, Mizuno K and Storz P: Protein kinase D1 regulates cofilin-mediated F-actin reorganization and cell motility through slingshot. Nat Cell Biol 11: 545-556, 2009.